

## Accepted Manuscript

Development of novel nano-biocomposite antioxidant films based on poly (lactic acid) and thymol for active packaging

Marina Ramos, Alfonso Jiménez, Mercedes Peltzer, María C. Garrigós

PII: S0308-8146(14)00571-8

DOI: <http://dx.doi.org/10.1016/j.foodchem.2014.04.026>

Reference: FOCH 15687

To appear in: *Food Chemistry*

Received Date: 10 September 2012

Revised Date: 27 March 2014

Accepted Date: 5 April 2014



Please cite this article as: Ramos, M., Jiménez, A., Peltzer, M., Garrigós, M.C., Development of novel nano-biocomposite antioxidant films based on poly (lactic acid) and thymol for active packaging, *Food Chemistry* (2014), doi: <http://dx.doi.org/10.1016/j.foodchem.2014.04.026>

This is a PDF file of an unedited manuscript that has been accepted for publication. As a service to our customers we are providing this early version of the manuscript. The manuscript will undergo copyediting, typesetting, and review of the resulting proof before it is published in its final form. Please note that during the production process errors may be discovered which could affect the content, and all legal disclaimers that apply to the journal pertain.

1     **Development of novel nano-biocomposite antioxidant films based on poly (lactic**  
2                                   **acid) and thymol for active packaging**

3  
4                   Marina Ramos\*, Alfonso Jiménez, Mercedes Peltzer, María C. Garrigós

5                   Analytical Chemistry, Nutrition & Food Sciences Department, University of Alicante

6                                   P.O. Box 99, 03080. Alicante, Spain

7                   Corresponding author. Tel. +34965903400x1187; fax. +34965903697.

8                                   E-mail address: marina.ramos@ua.es (M. Ramos)

9  
10    **Abstract**

11    Novel nano-biocomposite films based on poly (lactic acid) (PLA) were prepared by  
12    incorporating thymol, as the active additive, and modified montmorillonite (D43B) at  
13    two different concentrations. A complete thermal, structural, mechanical and functional  
14    characterization of all nano-biocomposites was carried out. Thermal stability was not  
15    significantly affected by the addition of thymol, but the incorporation of D43B  
16    improved mechanical properties and reduced the oxygen transmission rate by the  
17    formation of intercalated structures, as suggested by wide angle X-ray scattering  
18    patterns and transmission electron microscopy images. The addition of thymol  
19    decreased the PLA glass transition temperature, as the result of the polymer  
20    plasticization, and led to modification of the elastic modulus and elongation at break.  
21    Finally, the amount of thymol remaining in these formulations was determined by liquid  
22    chromatography (HPLC-UV) and the antioxidant activity by the DPPH spectroscopic  
23    method, suggesting that the formulated nano-biocomposites could be considered a  
24    promising antioxidant active packaging material.

25  
26    **Keywords:** PLA; active packaging; thymol; montmorillonite; antioxidant film.

27

28 **Introduction**

29 Poly (lactic acid) (PLA) is one of the most important commercially available bio-  
30 based and biodegradable thermoplastic polyesters (Inkinen, Hakkarainen, Albertsson &  
31 Sodergard, 2011). PLA can offer a sustainable alternative for food packaging across a  
32 wide range of commodity applications in response to consumers' demands and market  
33 trends in the use of renewable resources (Hughes, Thomas, Byun & Whiteside, 2012).  
34 PLA is a highly transparent and rigid material with a relatively low crystallization rate,  
35 making it a promising candidate for the fabrication of biaxial oriented films,  
36 thermoformed containers and stretch-blown bottles (Inkinen et al., 2011). However,  
37 some characteristic properties of pure PLA are inadequate for food packaging  
38 applications, such as weak thermal stability, low glass transition temperature, low gas  
39 barrier properties, and low ductility and toughness (Hwang et al., 2012). Recently, these  
40 poor PLA intrinsic properties have been improved by the reinforcement of the polymer  
41 matrix with layered silicates (Fukushima, Tabuani & Camino, 2009b; Gamez-Perez et  
42 al., 2011; Lagaron & Lopez-Rubio, 2011; Picard, Espuche & Fulchiron, 2011). In this  
43 sense, the incorporation of lamellar nanofillers with high aspect ratio, such as  
44 montmorillonites, has significantly enhanced mechanical, gas barrier, and optical  
45 properties (Rhim, Hong & Ha, 2009).

46 Current innovations in food packaging research include the development of active  
47 packaging systems based on materials, which can include a variety of additives such as  
48 antioxidants, antimicrobials, vitamins, flavours and colorants with the aim of improving  
49 their appearance and to extend foodstuff shelf-life (Álvarez, 2000; Del Nobile, Conte,  
50 Buonocore, Incoronato, Massaro & Panza, 2009; Gómez-Estaca, Giménez, Montero &  
51 Gómez-Guillén, 2009). The increasing demand for natural additives has resulted in

52 studies based on natural active compounds, such as plant extracts or essential oils,  
53 which are categorized as Generally Recognised as Safe (GRAS) by the US Food and  
54 Drug Administration as well as the current European Legislation for materials intended  
55 to be in contact with food (EU N10/2011 Regulation) (Ramos, Jiménez, Peltzer &  
56 Garrigós, 2012).

57 The addition of natural antioxidant additives allows their continued release during  
58 storage and distribution, extending food shelf-life by decreasing lipid auto-oxidation,  
59 which is recognized as a major cause of deterioration affecting both sensory and  
60 nutritional quality (Manzanarez-López, Soto-Valdez, Auras & Peralta, 2011). In this  
61 sense, thymol is a phenolic compound obtained from thyme and oregano essential oils  
62 that has been reported to be an effective antioxidant to reduce or eliminate lipid  
63 oxidation (Al-Bandak & Oreopoulou, 2007). Thymol antioxidant properties are due to  
64 its ability to donate H-atoms from phenol hydroxyl groups, which could react with  
65 peroxy radicals to produce stabilized phenoxyl radicals and, consequently, terminate  
66 lipid peroxidation chain reactions (Mastelic et al., 2008; Viuda-Martos, Navajas,  
67 Zapata, Fernández-López & Pérez-Álvarez, 2010). Several methods can be used to  
68 evaluate the antioxidant activity of natural additives as pure compounds or plant  
69 extracts, which are based on the measurement of the free radical scavenging ability  
70 (Sánchez-Moreno, 2002).

71 The development of different nanocomposites based on PLA with nanoclays  
72 (Fukushima et al., 2009b; Gamez-Perez et al., 2011; Picard et al., 2011) or active  
73 additives (Byun, Kim & Whiteside, 2010; López-Rubio & Lagaron, 2010; Hwang et al.,  
74 2012) has been extensively reported by several authors in the last years. However, few  
75 works have reported the combination of natural active additives and nanofillers in  
76 biopolymer matrices resulting in nano-biocomposites with antioxidant properties and

77 functionalities for use in food packaging applications. The use of these materials could  
78 be a promising alternative to enhance mechanical and gas barrier properties and extend  
79 foodstuff shelf-life.

80 This study focused on the development of antioxidant biodegradable films based on  
81 PLA reinforced with an organically modified montmorillonite [Dellite 43B (D43B)] and  
82 a natural additive (thymol) to obtain nano-biocomposites based on renewable resources  
83 with antioxidant activity and enhanced properties for active packaging applications. A  
84 full characterization was carried out including the determination of thermal, structural,  
85 mechanical and functional properties. Finally, the presence of thymol in the nano-  
86 biocomposites was determined by HPLC-UV analysis and antioxidant activity assessed  
87 by using the DPPH method.

88

## 89 **1. Materials and methods**

90

### 91 1.1. Materials

92 Poly (lactic acid) (PLA) 4060D was purchased in pellets from Natureworks Co.,  
93 (Minnetonka, MN, USA). Thymol (99.5 %), 2,2-Diphenyl-1-picrylhydrazyl (DPPH,  
94 95%) and methanol (HPLC grade) were supplied by Sigma-Aldrich (Madrid, Spain).

95 The nanoclay used was Dellite®43B (D43B) (Laviosa Chimica Mineraria S.p.A.  
96 Livorno, Italy). This nanoclay is a dimethyl-benzylidihydrogenated tallow ammonium  
97 modified montmorillonite; and it has a cation exchange capacity (CEC) of 95 meq/100 g  
98 clay, a bulk density of  $0.40 \text{ g cm}^{-3}$  and a typical particle size distribution between 7-9  
99  $\mu\text{m}$ .

100

### 101 1.2. Nano-biocomposites preparation

102 The different nano-biocomposites were obtained by melt-blending in a Haake  
103 Polylab QC mixer (ThermoFischer Scientific, Walham, MA, USA) with a mixing time  
104 of 20 min at 160 °C. Two different rotor speeds were used: 150 rpm in the loading and  
105 mixing steps and 100 rpm for the last 5 min, when thymol was added in order to limit  
106 degradation and to ensure the presence of the active additive in the final blends. Prior to  
107 the mixing step, PLA and the nanoclay were dried for 24 h at 80 °C and 100 °C,  
108 respectively. Thymol was used as received.

109 Five different formulations were obtained by adding thymol at one concentration  
110 level (8 wt%) and D43B at two different loadings (2.5 and 5 wt%), as described in  
111 Table 1. An additional sample without any additive was also prepared and used as  
112 control (neat PLA).

113 Films were obtained by compression-moulding at 180 °C in a hot-plates press  
114 (Carver Inc 3850, Wabash, IN, USA). Blends were kept at atmospheric pressure for 5  
115 min until melted and pressed at 2 MPa for 1 min, 3.5 MPa for 1 min and finally 5 MPa  
116 for 5 min to eliminate the trapped air bubbles. Transparent films were obtained with  
117 average thickness  $210 \pm 1 \mu\text{m}$  measured with a Digimatic Micrometer Series 293 MDC-  
118 Lite (Mitutoyo, Japan) at five random positions.

119

### 120 2.3. Thymol quantification

121 The actual amount of thymol in PLA films after processing was determined by solid-  
122 liquid extraction followed by liquid chromatography coupled to ultraviolet spectroscopy  
123 (HPLC-UV) analysis.  $0.05 \pm 0.01$  g of each film were extracted with 10 mL of methanol  
124 at 40 °C and 50 % relative humidity (RH) for 24 h in a climate chamber (Dycometal  
125 CM-081, Barcelona, Spain), as previously reported (Manzanarez-López et al., 2011).

126 Thymol was determined with a Shimadzu LC-20A liquid chromatograph (Kyoto,  
127 Japan) equipped with a UV detector at 274 nm. The column used was a LiChrospher  
128 100 RP 18 (250 mm x 5 mm x 5  $\mu\text{m}$ , Agilent Technologies, USA). The mobile phase  
129 was composed of acetonitrile and water (40:60) at 1 mL  $\text{min}^{-1}$  flow rate. 20  $\mu\text{L}$  of the  
130 extracted samples were injected and analyses were performed in triplicate.  
131 Quantification of the active additive was carried out by comparison of the  
132 chromatographic peak areas with standards in the same concentration range. Calibration  
133 curves were run at five concentrations from 100-500  $\text{mg Kg}^{-1}$  using appropriately  
134 diluted standards of thymol in methanol.

135 The antioxidant activity of thymol was analyzed using the stable radical 2,2-  
136 diphenyl-1-picrylhydrazyl (DPPH) as previously reported (Byun et al., 2010). This  
137 method is based on colour decay when the odd electron of the nitrogen atom in the  
138 DPPH radical is reduced by receiving one hydrogen atom from antioxidant compounds  
139 (Scherer & Godoy, 2009).

140 500  $\mu\text{L}$  of extracts were mixed with 2 mL of a methanolic solution of DPPH (0.06  
141 mM) in a capped cuvette. The mixture was shaken vigorously at room temperature and  
142 the absorbance of the solution was measured at 517 nm with a Biomate-3 UV-VIS  
143 spectrophotometer (Thermospectronic, Mobile, AL, USA). DPPH radical absorbs at 517  
144 nm but, upon reduction, its absorption at this particular wavelength decreases. The  
145 decay in absorbance was measured at 1 min intervals until it was stabilized (200 min).

146 All analyses were performed in triplicate.

147 The scavenging ability of the stable radical DPPH was calculated as percentage of  
148 inhibition (I %) with the equation (1):

$$149 \quad I(\%) = [(A_{Control} - A_{Sample}) / A_{Control}] \cdot 100 \quad (1)$$

150

151 where  $A_{Control}$  is the absorbance of the blank sample at  $t = 0$  min and  $A_{Sample}$  is the  
152 absorbance of the tested sample at  $t = 200$  min.

153

#### 154 2.4. Thermal analysis

155 Thermogravimetric analysis (TGA) tests were performed with a TGA/SDTA 851  
156 Mettler Toledo thermal analyzer (Schwarzenbach, Switzerland). Approximately 5 mg  
157 samples were heated from 30 °C to 700 °C at 10 °C min<sup>-1</sup> under nitrogen (flow rate 50  
158 mL min<sup>-1</sup>).

159 Differential scanning calorimetry (DSC) tests were used to determine glass transition  
160 temperatures ( $T_g$ ) of all materials using a TA DSC Q-2000 instrument (New Castle, DE,  
161 USA) under nitrogen atmosphere (flow rate 50 mL min<sup>-1</sup>). 3 mg samples were heated  
162 from -30 °C to 200 °C at 10 °C min<sup>-1</sup> (3 min hold), then cooled at 10 °C min<sup>-1</sup> to -30 °C  
163 (3 min hold) and further heating to 200 °C at 10 °C min<sup>-1</sup>.

164

#### 165 2.5. Mechanical properties

166 Tensile properties of all films were determined with a 3340 Series Single Column  
167 System Instron Instrument, LR30K model (Fareham Hants, UK) equipped with a 2 kN  
168 load cell. The main tensile parameters, such as elastic modulus and elongation at break,  
169 were calculated from stress-strain curves according to ASTM D882-09 Standard  
170 procedure (ASTM D 882 - 09. 2009). Before testing, all samples were conditioned for  
171 48 h at 25 °C and 50 % RH. Tests were performed with 100 x 10 mm<sup>2</sup> rectangular  
172 probes and initial grip separation of 60 mm. The specimens were stretched at 10 mm  
173 min<sup>-1</sup> until breaking. Results were the average of five measurements ( $\pm$  standard  
174 deviation).

175



## 176 2.6. Oxygen transmission rate (OTR)

177 OTR is defined as the quantity of oxygen circulating through a determined area of  
178 the parallel surface of a plastic film per time unit. An oxygen permeation analyzer (8500  
179 model Systech, Metrotec S.A, Spain) was used for OTR tests. Pure oxygen (99.9%) was  
180 introduced into the upper half of the diffusion chamber while nitrogen was injected into  
181 the lower half, where an oxygen sensor was located. Films were cut into 14 cm diameter  
182 circles for each formulation and they were clamped in the diffusion chamber at 25 °C  
183 before testing. Tests were performed in triplicate and mean values were expressed as  
184 oxygen transmission rate per film thickness (OTR·e).

185

## 186 2.7. Colour tests

187 Colour modifications on PLA films caused by the addition of the active additive and  
188 the nanoclay were followed by using a Konica CM-3600d COLORFLEX-DIFF2  
189 colorimeter, HunterLab, (Reston, VA, USA). Colour values were expressed as L\*  
190 (lightness), a\* (red/green) and b\* (yellow/blue) coordinates in the CIELab colour space.  
191 These parameters were determined at five different locations in films surfaces and the  
192 average values were calculated. Total colour difference ( $\Delta E^*$ ) was calculated according  
193 to Eq. (2).

194

$$195 \Delta E^* = [(\Delta L^*)^2 + (\Delta a^*)^2 + (\Delta b^*)^2]^{1/2} \quad (2)$$

196

197 where  $\Delta L^*$ ,  $\Delta a^*$  and  $\Delta b^*$  are the coordinate differences between control (neat PLA) and  
198 samples.

199

## 200 2.8. Morphological analysis

201 The nano-biocomposites structure, including the nanoclay dispersion, was studied by  
202 wide angle X-ray scattering (WAXS) patterns and transmission electron microscopy  
203 (TEM) micrographs.

204 WAXS patterns were recorded at room temperature in the scattering angle ( $2\theta$ ) 2-30°  
205 (step size: 0.01°, scanning rate: 8 s step<sup>-1</sup>) using filtered Cu K $\alpha$  radiation ( $\lambda$ : 1.54 Å). A  
206 Bruker D8-Advance model diffractometer (Madison, WI, USA) was used to determine  
207 the interlayer distance (d-spacing) and intercalation of the nanoclay.

208 TEM micrographs were performed using a JEOL JEM-2010 (Tokyo, Japan) with  
209 accelerating voltage 100 kV. Prior to analysis, films were ultra-microtomed to obtain  
210 slices of 100 nm thick (RMC, model MTXL).

211

### 212 **3. Results and discussion**

213

#### 214 3.1. Determination of thymol in nano-biocomposite films and antioxidant activity

215 The amount of thymol present in formulations after processing is indicated in Table  
216 1. Results showed that approximately 30 % of the initially thymol was lost during  
217 processing by evaporation or degradation due to the high temperature used during the  
218 polymer melting (Ramos et al., 2012). In this sense, other commonly used antioxidants  
219 in PLA-based formulations, such as butylated hydroxytoluene (BHT), suffer similar  
220 losses due to several factors, such as poor mixing in the extruder, evaporation, thermal  
221 degradation and the own antioxidant action of BHT to protect the polymer during  
222 processing (Ortiz-Vazquez, Shin, Soto-Valdez & Auras, 2011). Antioxidant volatility is  
223 desirable for food packaging to promote their migration from the polymer surface  
224 (Wessling, Nielsen, & Giacini, 2001). Therefore, thymol can be considered a good  
225 antioxidant in food packaging materials since most remains after processing and may be

226 released from the polymer matrix to improve food shelf-life. On the other hand, the  
227 amount of thymol after processing was slightly higher in nanocomposites containing  
228 D43B because the nanoclay can retard thymol evaporation during processing.

229 The antioxidant activity of the extracts obtained was estimated by scavenging  
230 activity against DPPH radicals. This test was performed to evaluate if the remaining  
231 thymol in the polymer matrix was enough to be considered an efficient antioxidant in  
232 these formulations. Results are also shown in Table 1. All extracts containing thymol  
233 showed an important antioxidant activity, as determined by the inhibition of the DPPH  
234 radical. The inhibition values are indicative of the amount of thymol remaining in the  
235 polymer matrix, which is able to act as an active (antioxidant) agent. In addition, thymol  
236 could protect the polymer matrix from oxidative degradation during processing and  
237 further the use of these nano-biocomposites (Ramos et al., 2012).

238

### 239 **Table 1**

240

### 241 3.2. Thermal analysis

242 Many authors have considered several molecular, as well as radical, mechanisms to  
243 explain PLA thermal degradation. The primary cause reported is a non-radical,  
244 'backbiting' ester interchange reaction involving -OH chain ends. This reaction  
245 mechanism can, depending upon the size of the cyclic transition state, produce lactide,  
246 oligomers or acetaldehyde as well as carbon monoxide. However, other authors have  
247 proposed radical reactions, which start with either alkyloxygen or acyl-oxygen  
248 homolysis leading to the formation of several types of oxygen- and carbon-centred  
249 macroradicals and carbon monoxide (Fukushima, Abbate, Tabuani, Gennari & Camino,  
250 2009a).

251 The thermal stability of all the materials was studied by TGA under nitrogen. Fig. 1  
252 shows the weight loss (TG) and derivative curves (DTG) obtained for PLA and all  
253 nano-biocomposites. The main degradation peak for PLA was observed in all samples  
254 around 365-370 °C. The first degradation step observed in those materials containing  
255 thymol was at 120 °C and continued up to 280 °C. Losses were associated with thymol  
256 degradation, as reported in previous works (Ramos et al., 2012). This result is another  
257 indication of the presence of thymol after processing. In this sense, the amounts of  
258 thymol, calculated by TGA (Table 2), were similar in all cases to values obtained from  
259 the quantification study discussed in the previous section. The initial degradation  
260 temperature ( $T_{ini}$ ), determined at 5% of weight loss, and maximum degradation  
261 temperature ( $T_{max}$ ) of the PLA degradation process are also shown in Table 2. No  
262 noticeable differences were observed for  $T_{ini}$  and  $T_{max}$  values in the materials studied.  
263 These results showed the addition of thymol and D43B did not significantly affect the  
264 nano-biocomposites thermal degradation profile.

265

266 **Fig. 1**

267

268 Glass transition temperatures ( $T_g$ ) in all nano-biocomposites were determined by  
269 DSC (Table 2). This parameter is dependent upon the polymer structural arrangement  
270 and corresponds to the torsion oscillation of the carbon backbone (Hughes et al., 2012).  
271  $T_g$  results showed the addition of D43B to PLA did not produce significant changes in  
272 the polymer structure, as reported by other authors (Lewitus, McCarthy, Ophir & Kenig,  
273 2006). The effect of thymol on PLA was much more important; thymol caused a  
274 decrease of more than 10 °C in  $T_g$  values, regardless of the presence of D43B. Similar  
275 behaviour was reported in PLA formulations with other antioxidants (Byun, Kim &

276 Whiteside, 2010; Hwang et al., 2012). This could be explained by the plasticizing effect  
277 caused by thymol resulting in an increase in molecular mobility of the macromolecular  
278 chains. Parameters related with crystallization or melting phenomena of PLA nano-  
279 biocomposites were not observed in these formulations due to the amorphous structure  
280 of the PLA used in this study.

281

## 282 **Table 2**

283

### 284 3.3. Mechanical properties

285 The addition of nanoclays to polymer matrices usually improves mechanical  
286 properties, particularly when nanoclay exfoliation occurs. Tensile tests were performed  
287 with all the materials studied to evaluate the influence on ductile properties. Results  
288 from elastic modulus (MPa) and elongation at break (%) are shown in Table 3. The  
289 addition of thymol to PLA matrices resulted in slight modifications of tensile properties.  
290 Elastic modulus decreased around 15 % from the original values for neat PLA for those  
291 materials containing thymol. This modification could be explained, again, by the  
292 plasticizing effect caused by thymol. This result confirmed the observed decrease in  $T_g$   
293 values already reported. Similar results have been reported for PLA and low-density  
294 polyethylene (LDPE) formulations with active compounds, such as resveratrol,  
295 carvacrol or  $\alpha$ -tocopherol (Hwang et al., 2012; Persico, Ambrogi, Carfagna, Cerruti,  
296 Ferrocino & Mauriello, 2009).

297

## 298 **Table 3**

299

300

301 As expected, the addition of D43B to PLA increased the elastic modulus and  
302 decreased elongation at break. Therefore, the addition of nanoclays increased brittleness  
303 (Tabatabaei & Aji, 2011). This behaviour is related to reinforcement provided by  
304 silicate layers and the high aspect ratio and surface area, good dispersion of clay layers  
305 throughout the polymer matrix, and strong interactions (Quilaqueo Gutiérrez,  
306 Echeverría, Ihl, Bifani & Mauri, 2012). However, this effect was not observed for  
307 ternary nano-biocomposites, where lower elastic modulus values were observed  
308 compared with pure PLA. This suggests the plasticizing effect of thymol in PLA may  
309 prevail over the reinforcement offered by the nanoclay.

310

#### 311 3.4. Oxygen transmission rate (OTR)

312 Barrier properties to oxygen of PLA nano-biocomposites were studied by the  
313 determination of oxygen transmission rate per film thickness ( $e$ ),  $OTR \cdot e$ . Results are  
314 shown in Table 3. A slight decrease in  $OTR \cdot e$  values for films containing D43B was  
315 observed. These results could be attributed to the effective intercalation of the nanoclay  
316 into the PLA matrix. This behaviour can be explained by considering that oxygen  
317 transmission rate is governed by two mechanisms: diffusion and sorption. In general,  
318 the efficient dispersion of D43B into the polymer matrix may form a tortuous pathway  
319 for oxygen molecules to permeate through the film. This more tortuous pathway results  
320 in oxygen molecules following a more complicated way through the polymer matrix. In  
321 general, the efficient dispersion of D43B into the polymer matrix may form a tortuous  
322 pathway for oxygen molecules to permeate through the film (Martino, Ruseckaite,  
323 Jiménez & Averous, 2010; Quilaqueo Gutiérrez et al., 2012).

324

325 Regarding PLA with thymol, a slight increase in the  $OTR \cdot e$  value was observed. The  
326 addition of thymol could modify the properties of PLA by increasing the mobility of  
327 macromolecular chains, reducing the polymer orientation and, consequently, decreasing  
328 oxygen permeability (Jamshidian, Arab Tehrani, Cleymand, Leconte, Falher &  
329 Desobry, 2012).

330 Finally, no significant differences were found in  $OTR \cdot e$  values for samples  
331 PLA/D43B2.5 and PLA/T/D43B2.5, containing D43B and thymol. However, sample  
332 PLA/T/D43B5 presented an  $OTR \cdot e$  value near to that obtained for PLA and higher than  
333 the one observed for sample PLA/D43B5, which may be due to decreased oxygen  
334 permeability caused by incorporation of thymol.

335 In general, the use of nanoclays in these PLA nano-biocomposites effectively  
336 improved oxygen barrier properties for food packaging applications.

### 338 3.5. Optical properties

339 Colour and transparency are important factors to be considered in food packaging  
340 since they could influence consumer acceptance and commercial success of a food  
341 product. Fig. 2 shows the visual aspect of all formulations. All the films had high  
342 transparency. Moreover, no agglomeration effects were revealed confirming the  
343 efficiency of the processing of PLA nanocomposites. However, some differences in the  
344 CIELab coordinates ( $L^*$ ,  $a^*$ ,  $b^*$ ) and  $\Delta E^*$  between neat PLA and nanocomposites were  
345 observed (Table 3). These differences could be attributed to the intrinsic colour of the  
346 additives used (white for thymol and yellowish for D43B). In this sense, pure PLA had  
347 the lowest  $L^*$  value, indicating that brightness increased with the addition of thymol and  
348 D43B. A yellowish-reddish tone was obtained for PLA/T, while PLA/T/D43B5 showed  
349 the higher value for  $\Delta E^*$ , as expected, due to the high concentrations of the additives

350 used (5 wt% D43B and 8 wt% thymol). The uniform distribution of the colour observed  
351 throughout the films (Fig. 2) also implies the additives were distributed uniformly  
352 within the polymer matrix. Similar tendencies in colour differences have been reported  
353 when using active additives such as  $\alpha$ -tocopherol and resveratrol into PLA, where the  
354 presence of these compounds contributed to strength of colour of the films obtained  
355 (Byun et al., 2010).

356

357 **Fig. 2**

358

359 3.6. Morphological analysis

360 3.6.1. Wide Angle X-Ray scattering (WAXS)

361 WAXS is a useful technique to determine d-spacing in intercalated nanocomposites.  
362 The WAXS pattern of PLA is characterized by a broad peak approximately at  $2\theta = 15^\circ$   
363 (Fukushima et al., 2009a), confirming its amorphous structure. No significant  
364 differences were found from the WAXS patterns of all the formulations studied at this  
365 angle range, indicating the polymer structure and crystallinity were not influenced by  
366 the presence of D43B and/or thymol.

367 The most significant features in this study were found in the low angle range ( $2-10^\circ$ ),  
368 (Figure 3). D43B is characterized by a single diffraction peak at  $2\theta = 4.6^\circ$   
369 corresponding to the (001) plane, accounting for a  $19.2 \text{ \AA}$  interlayer distance. A shift of  
370 the clay diffraction peak to lower angles, corresponding to an interlayer distance of  $35.6$   
371  $\text{ \AA}$ , was observed for all nano-biocomposites suggesting good interaction of D43B with  
372 the polymer matrix. Moreover, a significant decrease in peak intensity was observed,  
373 accounting for the formation of a disordered structure. These results indicate the  
374 formation of intercalated nano-biocomposites with PLA chains in the galleries of the



375 D43B layers (Picard et al., 2011). The basal diffraction observed at  $2\theta$  around  $5.2^\circ$  (d-  
376 spacing =  $17.0 \text{ \AA}$ ) in the nano-biocomposites WAXS patterns could be attributed to the  
377 fraction characterized by a different alkylammonium chain arrangement in the interlayer  
378 space (Persico et al., 2009).

379 The lowest peak intensity in the WAXS study was obtained for PLA/T/D43B2.5.  
380 The presence of thymol could favour nanoclay exfoliation and the effective interaction  
381 between the silicate layers and thymol, which could promote the swelling of the  
382 nanoclay stacks (Persico et al., 2009). However, the formulations with 5 wt% of D43B  
383 showed more intense peaks. This behaviour could be due to the unfavourable effect of  
384 nanoclay swelling, produced by thymol at high nanoclay loading. In conclusion, WAXS  
385 results suggest effective nanoclay intercalation achieved by mixing PLA with 2.5 wt%  
386 of D43B and 8 wt% of thymol.

387

388 **Fig. 3**

389

390 3.6.2. Transmission Electron Microscopy (TEM)

391 The dispersion of nanoclays in PLA nano-biocomposites was evaluated by TEM.  
392 Figure 4 shows the micrographs obtained for PLA/T/D43B2.5, showing the  
393 nanoparticles partial exfoliation. Single dispersed clay layers (dark regions in Figure 3)  
394 were randomly distributed through the PLA matrix (clear areas) and some regions with  
395 complete exfoliation of nanoclay layers were noticed. TEM analyses also suggested the  
396 good dispersion of D43B and thymol through the PLA matrix, already asserted by  
397 WAXS patterns, since no important aggregates were observed. The interaction of  
398 nanoclays with PLA was attributed to the formation of hydrogen bonds between the

399 carbonyl group of lactide and the hydroxyl groups of the nanoclay organic modifier  
400 (Fukushima et al., 2009b).

401

402 **Fig. 4**

403

#### 404 **4. Conclusions**

405 Different nano-biocomposite films, based on PLA, with antioxidant potential to be  
406 used in active packaging were processed and characterized. Several analytical  
407 techniques were used to evaluate the effects of incorporating the nanoclay (D43B) and  
408 thymol on the PLA nano-biocomposites properties. The addition of thymol did not  
409 significantly affect the thermal stability of PLA, but some decrease in the elastic  
410 modulus was observed due to the thymol plasticizing effect. The incorporation of D43B  
411 resulted in a clear enhancement of oxygen barrier and mechanical properties, due to the  
412 intercalation and partial exfoliation of the nanoparticles through the polymer matrix.  
413 Some differences in films colour were observed with the addition of thymol and D43B,  
414 but films remained mostly transparent. Most of the thymol added remained in the  
415 formulations after processing, which resulted in a significant antioxidant activity, as  
416 indicated by the high percentage of inhibition obtained using the DPPH test. In  
417 conclusion, the PLA nano-biocomposites studied, in particular those containing 8 wt%  
418 of thymol and 2.5 wt% of D43B, could be considered promising antioxidant active  
419 packaging materials with a biodegradable nature and able to increase foodstuff shelf-  
420 life.

421

422 **Acknowledgments**

423 Authors would like to thank the Spanish Ministry of Economy and Competitiveness for  
424 financial support (MAT2011-28468-C02-01) and Prof. Juan López Martínez  
425 (Polytechnic University of Valencia, Spain) and Prof. José M. Kenny (University of  
426 Perugia, Italy) for their support in experimental testing. Marina Ramos would like to  
427 thank University of Alicante (Spain) for UAFPU2011-48539721S pre-doctoral research  
428 grant.

429

430

ACCEPTED MANUSCRIPT

431 **References**

432

433 (ASTM D 882 - 09. 2009). Standard test method for tensile properties of thin plastic sheeting In: 468  
434 Annual book of ASTM standards. Amer. Soc. for Testing & Materials, Philadelphia, PA.

435 Al-Bandak, G., & Oreopoulou, V. (2007). Antioxidant properties and composition of *Majorana syriaca*  
436 extracts. *European Journal of Lipid Science and Technology*, 109(3), 247-255.

437 Álvarez, M. F. (2000). Revisión: Envasado activo de los alimentos / Review: Active food packaging Food  
438 Science and Technology International, 6(2), 97-108.

439 Byun, Y., Kim, Y. T., & Whiteside, S. (2010). Characterization of an antioxidant polylactic acid (PLA)  
440 film prepared with  $\alpha$ -tocopherol, BHT and polyethylene glycol using film cast extruder. *Journal of*  
441 *Food Engineering*, 100(2), 239-244.

442 Del Nobile, M. A., Conte, A., Buonocore, G. G., Incoronato, A. L., Massaro, A., & Panza, O. (2009).  
443 Active packaging by extrusion processing of recyclable and biodegradable polymers. *Journal of*  
444 *Food Engineering*, 93(1), 1-6.

445 Fukushima, K., Abbate, C., Tabuani, D., Gennari, M., & Camino, G. (2009a). Biodegradation of  
446 poly(lactic acid) and its nanocomposites. *Polymer Degradation and Stability*, 94(10), 1646-1655.

447 Fukushima, K., Tabuani, D., & Camino, G. (2009b). Nanocomposites of PLA and PCL based on  
448 montmorillonite and sepiolite. *Materials Science and Engineering: C*, 29(4), 1433-1441.

449 Gamez-Perez, J., Nascimento, L., Bou, J. J., Franco-Urquiza, E., Santana, O. O., Carrasco, F., & Ll.  
450 MasPOCH, M. (2011). Influence of crystallinity on the fracture toughness of poly(lactic  
451 acid)/montmorillonite nanocomposites prepared by twin-screw extrusion. *Journal of Applied*  
452 *Polymer Science*, 120(2), 896-905.

453 Gómez-Estaca, J., Giménez, B., Montero, P., & Gómez-Guillén, M. C. (2009). Incorporation of  
454 antioxidant borage extract into edible films based on sole skin gelatin or a commercial fish gelatin.  
455 *Journal of Food Engineering*, 92(1), 78-85.

456 Hughes, J., Thomas, R., Byun, Y., & Whiteside, S. (2012). Improved flexibility of thermally stable poly-  
457 lactic acid (PLA). *Carbohydrate Polymers*, 88(1), 165-172.

458 Hwang, S. W., Shim, J. K., Selke, S. E. M., Soto-Valdez, H., Matuana, L., Rubino, M., & Auras, R.  
459 (2012). Poly(L-lactic acid) with added  $\alpha$ -tocopherol and resveratrol: optical, physical, thermal and  
460 mechanical properties. *Polymer International*, 61(3), 418-425.

- 461 Inkinen, S., Hakkarainen, M., Albertsson, A.-C., & Sodergard, A. (2011). From Lactic Acid to Poly(lactic  
462 acid) (PLA): Characterization and Analysis of PLA and Its Precursors. *Biomacromolecules*, 12(3),  
463 523-532.
- 464 Jamshidian, M., Arab Tehrani, E., Cleymand, F., Leconte, S., Falher, T., & Desobry, S. (2012). Effects of  
465 synthetic phenolic antioxidants on physical, structural, mechanical and barrier properties of poly  
466 lactic acid film. *Carbohydrate Polymers*, 87(2), 1763-1773.
- 467 Lagaron, J. M., & Lopez-Rubio, A. (2011). Nanotechnology for bioplastics: opportunities, challenges and  
468 strategies. *Trends in Food Science & Technology*, 22(11), 611-617.
- 469 Lewitus, D., McCarthy, S., Ophir, A., & Kenig, S. (2006). The Effect of Nanoclays on the Properties of  
470 PLLA-modified Polymers Part 1: Mechanical and Thermal Properties. *Journal of Polymers and the  
471 Environment*, 14(2), 171-177.
- 472 López-Rubio, A., & Lagaron, J. M. (2010). Improvement of UV stability and mechanical properties of  
473 biopolyesters through the addition of  $\beta$ -carotene. *Polymer Degradation and Stability*, 95(11), 2162-  
474 2168.
- 475 Manzanarez-López, F., Soto-Valdez, H., Auras, R., & Peralta, E. (2011). Release of [alpha]-Tocopherol  
476 from Poly(lactic acid) films, and its effect on the oxidative stability of soybean oil. *Journal of Food  
477 Engineering*, 104(4), 508-517.
- 478 Martino, V. P., Ruseckaite, R. A., Jiménez, A., & Averous, L. (2010). Correlation between Composition,  
479 Structure and Properties of Poly(lactic acid)/Polyadipate-Based Nano-Biocomposites.  
480 *Macromolecular Materials and Engineering*, 295(6), 551-558.
- 481 Mastelic, J., Jerkovic, I., Blazevic, I., Poljak-Blazi, M., Borovic, S., Ivancic-Bace, I., Smrecki, V.,  
482 Zarkovic, N., Brcic-Kostic, K., Vikić-Topić, D., & Müller, N. (2008). Comparative study on the  
483 antioxidant and biological activities of carvacrol, thymol, and eugenol derivatives. *Journal of  
484 Agricultural and Food Chemistry*, 56(11), 3989-3996.
- 485 Ortiz-Vazquez, H., Shin, J., Soto-Valdez, H., & Auras, R. (2011). Release of butylated hydroxytoluene  
486 (BHT) from Poly(lactic acid) films. *Polymer Testing*, 30(5), 463-471.
- 487 Persico, P., Ambrogi, V., Carfagna, C., Cerruti, P., Ferrocino, I., & Mauriello, G. (2009). Nanocomposite  
488 polymer films containing carvacrol for antimicrobial active packaging. *Polymer Engineering &  
489 Science*, 49(7), 1447-1455.

- 490 Picard, E., Espuche, E., & Fulchiron, R. (2011). Effect of an organo-modified montmorillonite on PLA  
491 crystallization and gas barrier properties. *Applied Clay Science*, 53(1), 58-65.
- 492 Quilaqueo Gutiérrez, M., Echeverría, I., Ihl, M., Bifani, V., & Mauri, A. N. (2012).  
493 Carboxymethylcellulose–montmorillonite nanocomposite films activated with murta (*Ugni molinae*  
494 Turcz) leaves extract. *Carbohydrate Polymers*, 87(2), 1495-1502.
- 495 Ramos, M., Jiménez, A., Peltzer, M., & Garrigós, M. C. (2012). Characterization and antimicrobial  
496 activity studies of polypropylene films with carvacrol and thymol for active packaging. *Journal of*  
497 *Food Engineering*, 109(3), 513-519.
- 498 Rhim, J.-W., Hong, S.-I., & Ha, C.-S. (2009). Tensile, water vapor barrier and antimicrobial properties of  
499 PLA/nanoclay composite films. *LWT - Food Science and Technology*, 42(2), 612-617.
- 500 Sánchez-Moreno, C. (2002). Review: methods used to evaluate the free radical scavenging activity in  
501 foods and biological systems. *Food Science and Technology International*, 8(3), 121-137.
- 502 Scherer, R., & Godoy, H. T. (2009). Antioxidant activity index (AAI) by the 2,2-diphenyl-1-  
503 picrylhydrazyl method. *Food Chemistry*, 112(3), 654-658.
- 504 Tabatabaei, S. H., & Aji, A. (2011). Orientation, mechanical, and optical properties of poly (lactic acid)  
505 nanoclay composite films. *Polymer Engineering & Science*, 51(11), 2151-2158.
- 506 Viuda-Martos, M., Navajas, Y. R., Zapata, E. S., Fernández-López, J., & Pérez-Álvarez, J. A. (2010).  
507 Antioxidant activity of essential oils of five spice plants widely used in a Mediterranean diet.  
508 *Flavour and Fragrance Journal*, 25(1), 13-19.
- 509
- 510

511 **Figure captions**

512 **Fig. 1.** TG (a) and DTG (b) curves obtained for pure PLA and nano-biocomposites  
513 under nitrogen.

514 **Fig. 2.** Visual observation of PLA and nano-biocomposite films.

515 **Fig. 3.** WAXS patterns of D43B, PLA and nano-biocomposites.

516 **Fig. 4.** TEM images of PLA/T/D43B2.5 nano-biocomposite film.

ACCEPTED MANUSCRIPT

**Table 1**

Quantification of thymol by HPLC-UV analysis and radical scavenging activity measured by DPPH assay obtained for the different formulations used in this work.

Sample	D43B (wt%)	Thymol (wt%)	Amount of extracted Thymol (wt%) <sup>a</sup>	Inhibition (%) <sup>b</sup>
PLA	-	-	n.d.	n.d.
PLA/D43B2.5	2.5	-	n.d.	n.d.
PLA/D43B5	5	-	n.d.	n.d.
PLA/T	-	8	5.57 ± 0.01	71.1 ± 0.2
PLA/T/D43B2.5	2.5	8	5.99 ± 0.03	84.3 ± 0.3
PLA/T/D43B5	5	8	5.78 ± 0.02	83.5 ± 0.1

<sup>a</sup>(n =3, mean ± SD); <sup>b</sup>(n =3, mean ± SD); (n.d.: not detected)



**Table 2**

TGA and DSC parameters obtained for all nano-biocomposites.

Sample	wt% weight loss (1 <sup>st</sup> step)	T <sub>ini</sub> (°C) (2 <sup>nd</sup> step)	T <sub>max</sub> (°C) (2 <sup>nd</sup> step)	T <sub>g</sub> (°C)
PLA	n.d.	335	369	57
PLA/D43B2.5	n.d.	334	363	57
PLA/D43B5	n.d.	340	369	57
PLA/T	6.6	331	366	43
PLA/T/D43B2.5	6.3	336	366	41
PLA/T/D43B5	7.1	339	369	44

(n.d.: not detected)

**Table 3**

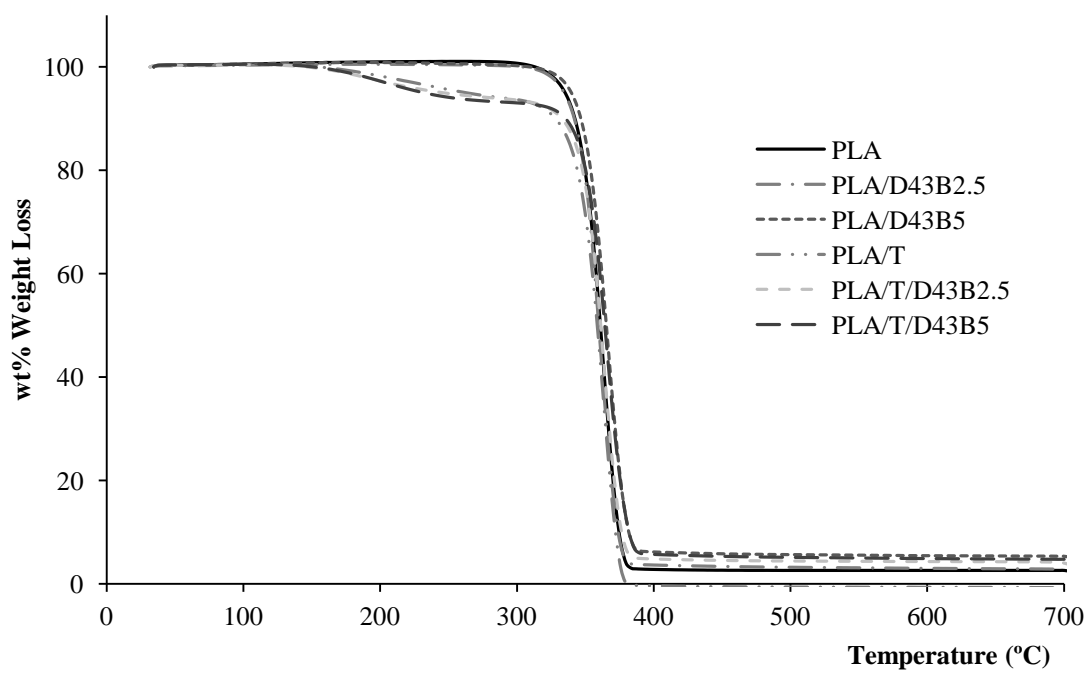
Tensile properties (ASTM D882-09), oxygen transmission rate and CIELab colour parameters obtained for all the studied formulations.

Sample	Elongation at break (%) <sup>a</sup>	Elastic modulus (MPa) <sup>a</sup>	OTR·e (cm <sup>3</sup> mm m <sup>-2</sup> day) <sup>b</sup>	L*	a*	b*	ΔE* <sup>c</sup>
PLA	3.5 ± 0.1	2575 ± 76	22.1 ± 1.5	30.3	-0.11	-0.20	-
PLA/D43B2.5	2.1 ± 0.4	2739 ± 151	20.1 ± 2.0	30.7	0.02	-0.01	0.5
PLA/D43B5	1.5 ± 0.2	2715 ± 95	17.1 ± 2.3	32.0	-0.24	-0.81	1.9
PLA/T	4.3 ± 0.1	2167 ± 196	23.0 ± 0.2	33.3	-0.49	-1.10	3.2
PLA/T/D43B2.5	2.4 ± 0.1	2246 ± 135	20.1 ± 0.1	32.0	-0.22	-1.14	2.0
PLA/T/D43B5	2.4 ± 0.2	2140 ± 116	22.7 ± 1.3	34.4	-0.58	-1.48	4.4

<sup>a</sup> n = 5, mean ± SD  
<sup>b</sup> n = 3, mean ± SD (e: thickness, mm)  
<sup>c</sup> PLA film was used as control

Fig. 1

(a)



(b)

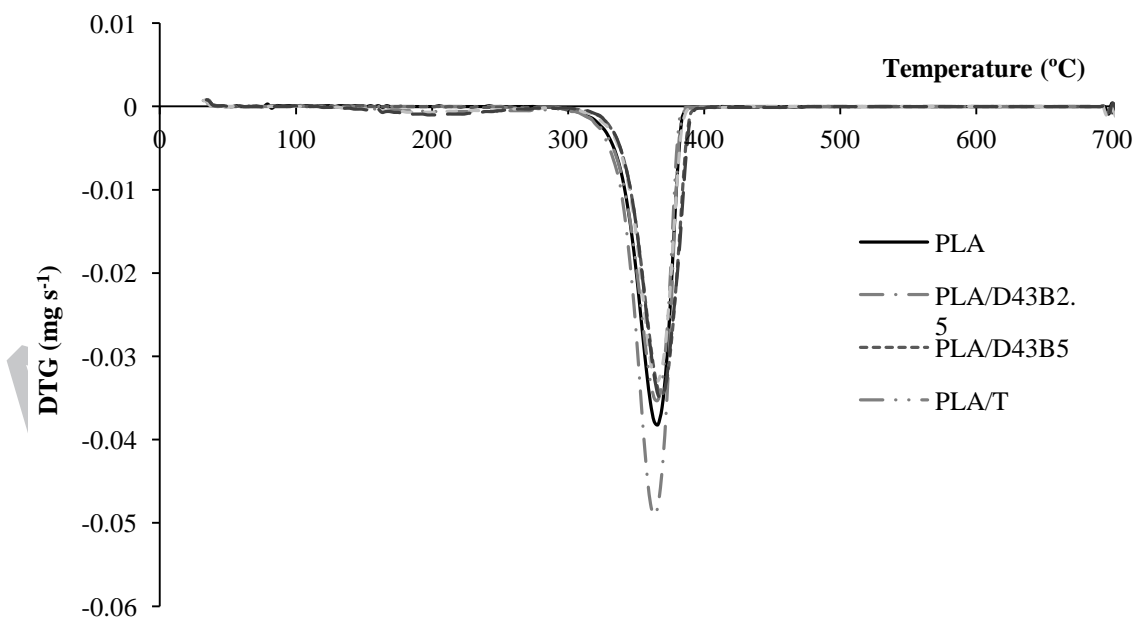


Fig. 2

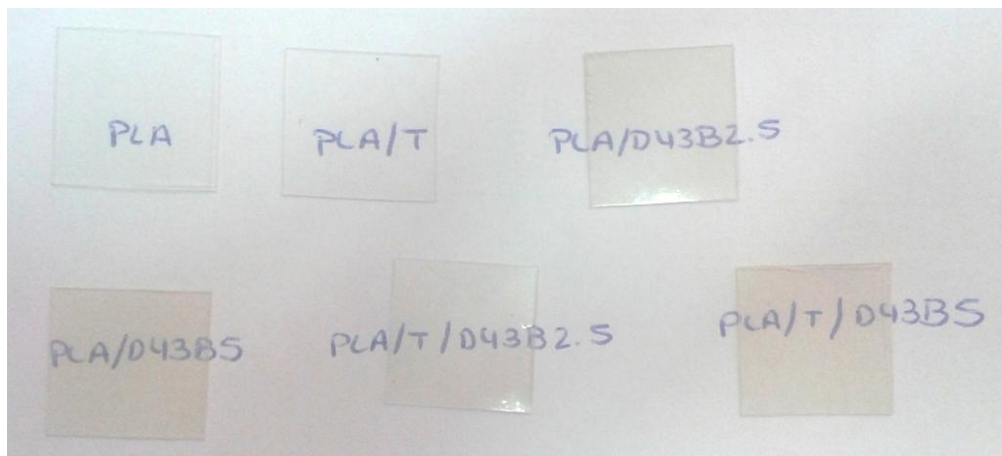


Fig. 3

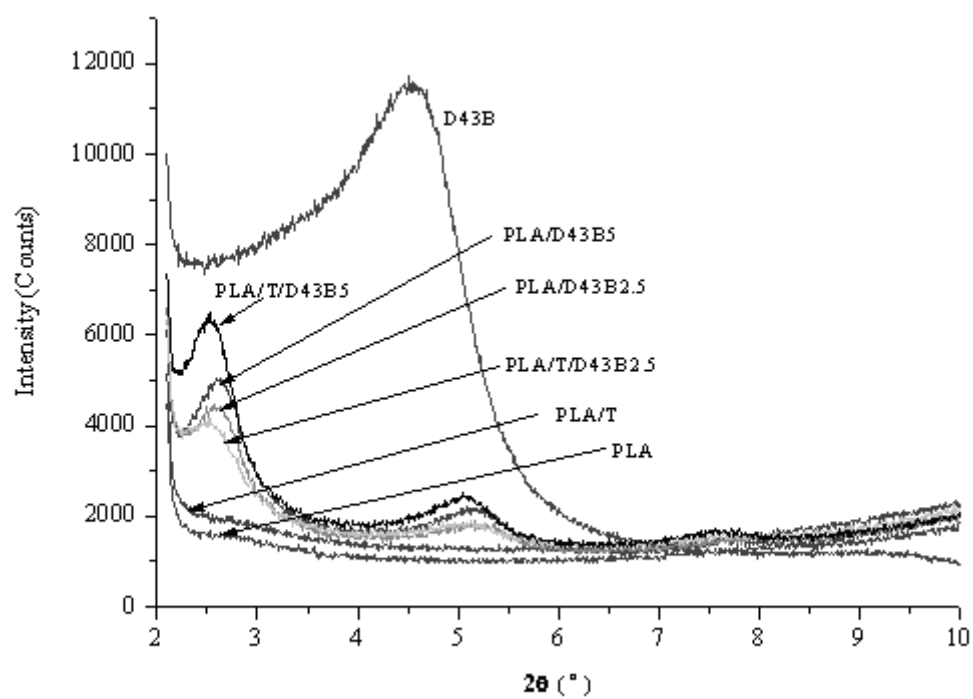
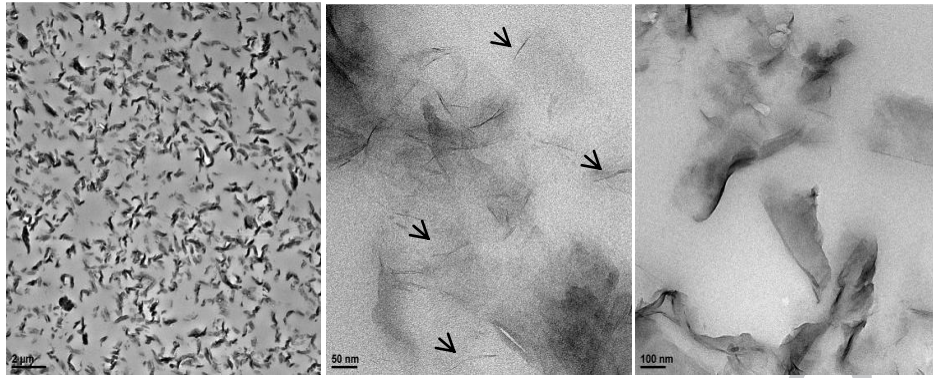


Fig. 4



## Highlights

1. Thymol and D43B were added to PLA to get antioxidant nano-biocomposite films
2. A full characterization of all formulations was carried out
3. The presence of thymol in the films and its antioxidant activity were demonstrated
4. The addition of D43B improved oxygen barrier and mechanical properties of films
5. The film with thymol and 2.5 wt% of D43B was considered the best enhanced material